Journal of Solid State Chemistry 183 (2010) 2501–2505

Contents lists available at ScienceDirect

Journal of Solid State Chemistry

journal homepage: www.elsevier.com/locate/jssc

Rapid Communication

Transport properties, specific heat and thermal conductivity of GaN nanocrystalline ceramic

Czesław Sułkowski [a], Andrzej Chuchmała [b,*], Andrzej J. Zaleski [a], Marcin Matusiak [a], Jan Mucha [a], Paweł Głuchowski [a], Wiesław Stręk [a]

[a] Institute of Low Temperature and Structure Research, Polish Academy of Sciences, P.O. Box 1410, 50-950 Wroclaw, Poland
[b] Wroclaw University of Technology, Institute of Electrical Engineering Fundamentals (I7), Wybrzeze Wyspianskiego 27, 50-370 Wroclaw, Poland

ARTICLE INFO

Article history:
Received 18 June 2010
Received in revised form
28 July 2010
Accepted 31 July 2010
Available online 5 August 2010

Keywords:
Nanoceramics
GaN
Amorphisation
Core-shell

ABSTRACT

The structural and transport properties (resistivity, thermopower and Hall effect), specific heat and thermal conductivity have been measured for GaN nanocrystalline ceramic prepared by hot pressing. It was found that the temperature dependence of resistivity in temperature range 10–300 K shows the very low activation energy, which is ascribed to the shallow donor doping originating in amorphous phase of sample. The major charge carriers are electrons, what is indicated by negative sign of Hall constant and Seebeck coefficient. The thermopower attains large values (-58 μV/K at 300 K) and was characterized by linear temperature dependence which suggests the diffusion as a major contribution to Seebeck effect. The high electron concentration of 1.3×10^{19} cm^{-3} and high electronic specific heat coefficient determined to be 2.4 mJ/molK^2 allow to conclude that GaN ceramic demonstrates the semimetallic-like behavior accompanied by very small mobility of electrons ($\sim$0.1 cm^2/V s) which is responsible for its high resistivity. A low heat conductivity of GaN ceramics is associated with partial amorphous phase of GaN grains due to high pressure sintering.

© 2010 Elsevier Inc. All rights reserved.

1. Introduction

In the last decade nanomaterials gain significant attention due to their unusual physical and chemical properties resulting from the size effects [1–3]. Especially dense ceramics with nanometric grains are useful in wide area of applications such as transparent armor [4] or solid oxide fuel cells [5,6]. Gallium nitride (GaN) has been widely investigated mainly as an optical material because of wide and direct band gap [7], what pretends this material as an excellent optical material in the field of blue lasers [8,9], optical and electrooptical devices [10,11]. Very recently the exploitation of intrinsic electric fields to enhance room-temperature doping in order to obtain excellent efficiency of deep UV laser emission was demonstrated [12]. The defects and inner band gap energy levels could lead to emission in various regions of visible spectrum [13], with strong influence of grain dimensions [14,15]. Generally, GaN represents excellent electronic transport properties such as high breakdown voltage and very high charge carriers mobility. They were utilized in construction of transistors for high output-power levels circuits especially in telecommunications industry.

Apart their optoelectronic applications the GaN systems demonstrate interesting thermoelectric properties. The thermopower measurements of GaN crystalline thin films were reported by Liu and Balandin [16], which indicate possible thermoelectric applications.

The synthesis and optical properties of GaN nanocrystalline powders were reported by several authors [17–19]. The room-temperature ferromagnetic properties of GaN nanocrystalline powders were reported by Madhu et al. [20], which suggest that such materials may find application in spintronics.

Densification of fine grain ceramics deal with serious obstacles related to the significant grain growth during sintering. There are few methods for fabrication of dense ceramics with nanometric grains such as spark plasma sintering [21–23] or low temperature high pressure (LTHP) method [24]. In the former case the grain growth is suppressed by heating of powders only close to the grain boundaries with very short electric pulses, whereas the latter one is based on the application of short heating cycle with applied high pressure (up to several GPa).

Recently the superconductivity and magnetic properties of GaN ceramics sintered from nanocrystalline powders by low temperature high pressure (LTHP) technique were reported by Zaleski et al. [25]. The GaN ceramics under investigation were characterized by metallic black color resulting presumably from cation and anion defects. According to Larson and Satpathy [26], Ga vacancies are responsible for the magnetism in GaN crystal. The metallic black color of GaN ceramics allowed us to presume that they may be characterized by interesting electronic properties.

* Corresponding author.
E-mail address: andrzej.chuchmala@pwr.wroc.pl (A. Chuchmała).

0022-4596/$ - see front matter © 2010 Elsevier Inc. All rights reserved.
doi:10.1016/j.jssc.2010.07.052

In the present work we report the detailed studies of transport properties of dense GaN ceramics prepared by LTHP method at 4 GPa.

2. Experimental

The preparation procedure of GaN nanopowders was divided into two main steps—the first one is the hydrothermal processing using a microwave reactor and the second is the synthesizing of GaN nanocrystalline powder using a horizontal quartz reactor. This is a modification of method reported in our previous paper [12]. Hydrothermal processing using microwaves as stimulators and accelerators of the conversion of Ga_2O_3 (Alfa Aesar 99.999%) into $Ga(NO_3)_3$ was applied. The most important improvement in comparison to already operated hydrothermal reactors was done by applying microwaves as a heater. The waveguide is placed outside the reaction area and thus protected the reactants from contact with the heater elements. The Ga_2O_3 and HNO_3 were moved into the Teflon vessel; afterwards deionized water was added. Finally the prepared solution was placed in the microwave reactor (ERTEC MV 02-02).

After hydrothermal processing at 300 °C under pressure lower than 20 atm, a solution of $Ga(NO_3)_3$ was obtained. The solution was carefully dried in an oven with gradually increasing the temperature from 70 to 200 °C. Then, the obtained powder was placed in an alumina crucible and inserted into a quartz tube (24 mm inside diameter) and was calcined at 600 °C for 6 h in air flow to convert $Ga(NO_3)_3$ into Ga_2O_3. The crushed powder samples were placed at room temperature in a quartz tube in NH_3 flow and after pouring, the material was heated to the required temperature of 1050 °C, in which was kept for 3.5 h. The NH_3 vapor (99.85% vol.) used for nitridation was additionally purified by passing it over a zeolite trap. The GaN nanocrytalline yellow powders were milled in an agate mortar and then hot-pressed into black color pellet under 4 GPa at 800 °C for 1 min (LTHP method). In order to determine the structure of the powders and ceramics, the X-ray diffraction (XRD) measurements were performed.

For GaN ceramics samples transport properties (resistivity, thermopower and Hall effect) and specific heat have been measured. The resistivity measurements were performed by standard four-probe method in the temperature range 10–300 K. Thermoelectric power was determined in the temperature range 7–300 K by steady-state mode using a semiautomatic instrument fitted into the transport liquid-helium Dewar [27]. The sample was clamped between two spring-loaded Cu blocks with attached heaters. A pair of platinum thermometers (HY-CAL Engineering EL-700-K, Pt—1000 Ω) was used to detect the temperature differences between the blocks. The blocks were insulated from the surrounding so that the temperature difference could be produced by the heaters. The quality of thermal contact between the sample and the Cu blocks was tested by electrical resistance measurements and only values below 20 Ω were accepted. A calibration of the equipment was performed using Pb(6 N) sample [28]. Hall effect measurements were performed on sample pressed under 4 GPa of ~0.5 mm thickness in a magnetic field of 13 T and in temperature range 70–300 K. The specific heat measurements in range 5–300 K were carried out in adiabatic calorimeter (PPMS Quantum Design).

3. Results and discussion

3.1. Structure and morphology

The XRD patterns of GaN nanocrystalline powder and ceramics show the diffraction peaks that could be ascribed to the formation of hexagonal GaN with a wurtzite-type structure (Fig. 1). The mean grain size of GaN nanocrystals has been determined by the Scherrer formula applied to the (110) peak. A substantial decrease of the mean grain size has been observed in sample pressed under 4 GPa in comparison with green body, which equals to 10.3 and 21.3 nm, respectively.

Such significant decrease of the mean grain size is associated with partial distortion of crystallographic structure of GaN nanocrystalline grains. Within the core-shell model assuming spherical shape of nanocrystals, it may be treated as composed from the crystalline core and strongly distorted shell which is amorphous-like phase. The GaN ceramics may be modeled as a composite material schematically illustrated in Fig. 2.

It indicates the partial amorphous phase of GaN grain which emerged in the vicinity of grain boundaries. This resulted in some kind of 'composite' material comprising of crystalline, nanometric grains embedded in amorphous matrix. The fraction of volume occupied by the crystalline phase, V_c, could be determined as $V_c/V=(r/R)^3$ assuming the spherical shape of nanograins with R for

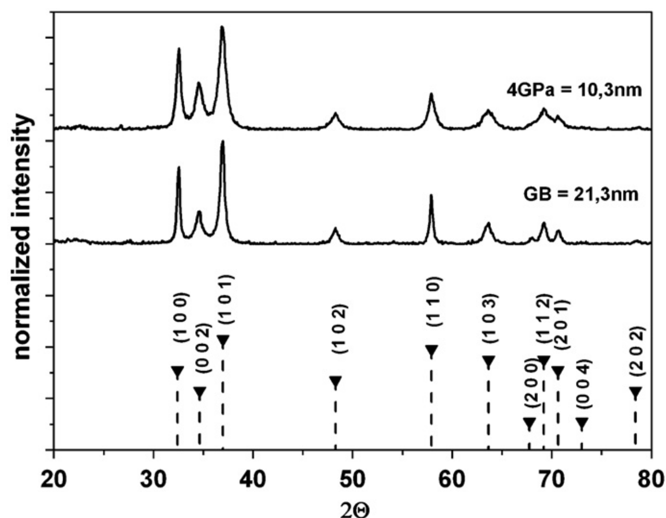

Fig. 1. XRD patterns of GaN ceramics sintered at 4 GPa and respective nanopowder.

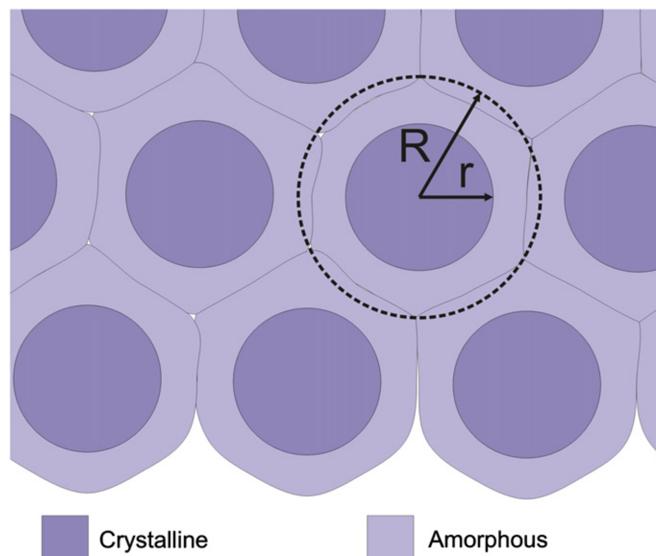

Fig. 2. The model of crystallite-amorphous core-shell structure of nanocrystalline ceramic.

powders and r for ceramics. From this formula one could obtain that crystalline phase consists of ~13% of sample.

3.2. Electrical resistivity

The temperature dependence of resistivity of GaN ceramic was measured in a temperature range 10–300 K. It is illustrated in Fig. 3.

One can see that in general it shows the semiconductor-like behavior, i.e. the resistivity increases with decreasing temperature. The resistivity for GaN nanocrystalline ceramic demonstrates much higher values compared to n-type GaN films [29], where it was determined to be of the order of 0.1 Ω cm at 300 K. The high resistivity for our GaN sample (7.4 Ω cm) seems to be connected with extremely low mobility of electrons (~0.1 cm^2/V s) as will be show later.

The temperature dependence of resistivity of semiconductors is usually fitted by [30]

$$\rho(T) = \rho_0 \exp\left(\frac{E_g}{2k_BT}\right), \quad (1)$$

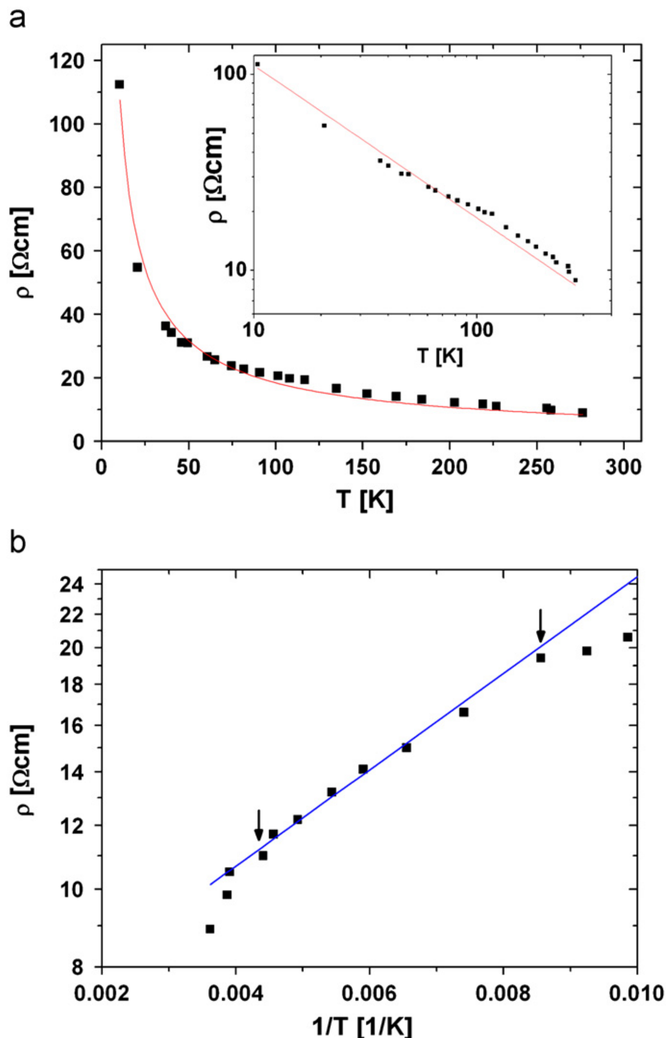

Fig. 3. (a) The temperature dependence of electrical resistivity, $\rho(T)$, of GaN ceramic. Inset shows the resistivity vs. temperature with log–log scale. Linear dependence is clearly seen. (b) Dependence of $\rho(T)$ vs. $1/T$. In temperature range (~120–220 K) the dependence is linear, hence energy gap, E_g, was determined (see text).

where E_g is the band gap energy, k_B the Boltzmann constant and T the temperature. Fitting of experimental data is not perfect (see Fig. 3(b)) and gives E_g~23.8 meV in temperature range 120–220 K. It indicates that the thermal activation of charge carriers may be effective only in limited temperature range. E_g values are about 2 orders of magnitude lower than for single crystal GaN, so it is hardly to ascribe such large change only by effect of small grains size. Taking into account the crystalline-amorphous structure of investigated sample, additional energetic levels in forbidden band should emerges due to formation of trapping centers as a consequence of amorphization. Then E_g is the distance between the shallow donor levels (as we shall see in analysis below, the electrons are major charge carriers) and conduction band. However, the question whether these levels forming impurity band inside the band gap of material, remains open at the present stage of investigations.

In temperature range 120–220 K, the thermal energy k_BT is much smaller than E_g (k_BT=18.9 meV at 220 K and k_BT=10.3 meV at 120 K), that confirms semiconducting character of the sample.

On the other hand a quite satisfactory fitting of temperature dependence of resistivity was obtained by using the power-like expression $\rho = AT^n$ (Fig. 3(a)), which may be applied for granular ceramics [31]. The power factor $n = -0.778$ and is very close to $-3/4$, which originates from variable range conductivity. However, in sample under investigations the charge concentration is very high, as we shall show in later sections, thus this issue needs further investigations in order to determine the details of such behavior.

3.3. Thermoelectric power

The measurements of thermoelectric properties are very useful to study the electrical conductivity of metallic and semiconductor materials. The temperature dependence of thermopower expressed by Seebeck coefficient was measured in temperature range 7–300 K. The results are depicted in Fig. 4. One can see that the thermoelectric power S increases in magnitude almost linearly with temperature. The negative value of Seebeck coefficient may be attributed to electrons as major charge carriers (n-type conductivity) and its linear dependence indicates very low contribution of phonon-drag to the Seebeck effect.

From obtained results it is possible to extract the carriers' density at Fermi level from the formula within the free electron

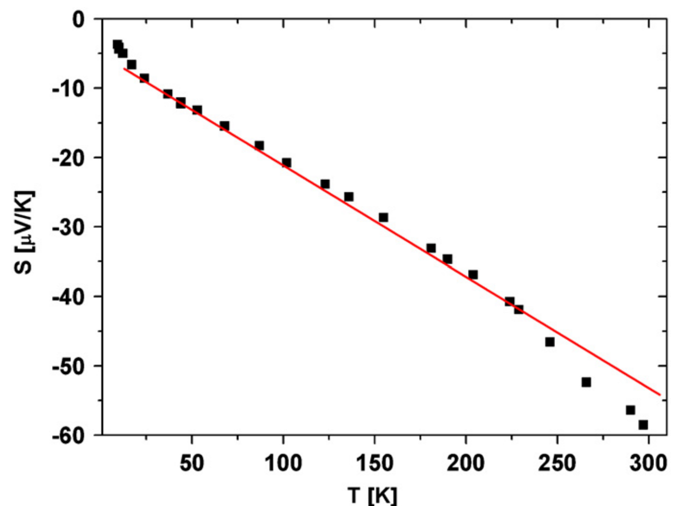

Fig. 4. The temperature dependence of thermopower, $S(T)$, for GaN nanocrystalline ceramic sintered at 4 GPa.

model

$$S(T) = \frac{3\pi^2 k_B^2}{2e} \frac{g(E_F)}{n} T, \quad (2)$$

where the $g(E_F)$ is the density of states at Fermi level, n the carriers concentration, e the elementary charge, k_B the Boltzmann constant and T the temperature. The fitting of above formula to the obtained results gives the value of $g(E_F)/n$ equal to 3.65 eV^{-1}, which corresponds to $g(E_F)$ of the order of 5×10^{-4} eV^{-1} per unit cell.

The Seebeck coefficient of wurzite GaN crystal at room temperature calculated by Liu and Balandin [16] was higher in magnitude ($S \approx -250$ μV/K) as in our experiment.

3.4. Hall effect

To determine the electron concentration n_H in GaN ceramics the Hall effect measurements were performed. Fig. 5 shows the temperature dependence $n_H(T) = -1/R_H(T)e$, where e is electronic charge and $R_H(T)$ is Hall coefficient. Its magnitude at room temperature was found to be 1.3×10^{19} cm^{-3}, which is almost one order higher than that for GaN thin films ($\sim 1.5 \times 10^{18}$ cm^{-3}) [32]. The observed decreasing of n_H with temperature is here considerably lower than for semiconductors. Using values of the ρ and R_H, an effective electron mobility $\mu = R_H/\rho$ was determined to be $\mu \sim 0.1$ $cm^2/V\,s$ (inset in Fig. 5). This value is extremely low in comparison to that one measured by Look et al. [32] (600 $cm^2/V\,s$) and it may be connected with vast amount of scattering centers aggregated in amorphous phase.

3.5. Specific heat

Fig. 6 shows dependence of C/T vs. T^2 in low temperature range. From the data, electronic specific heat coefficient, $\gamma = 2.4$ $mJ/molK^2$, was determined. The large value of γ is similar as for non-transition metals, and proves also that metallic phase occupies large part of volume of the sample. For sufficiently low temperature, $T \ll \Theta$, Debye model for lattice specific heat, C_l, can be applied to determine Debye temperature, Θ, according with formula

$$C_l = 234 N n k_B \left(\frac{T}{\Theta}\right)^3, \quad (3)$$

where N is the Avogadro number, $n = 2$ the number of atoms in the GaN chemical formula unit and k_B the Boltzmann constant.

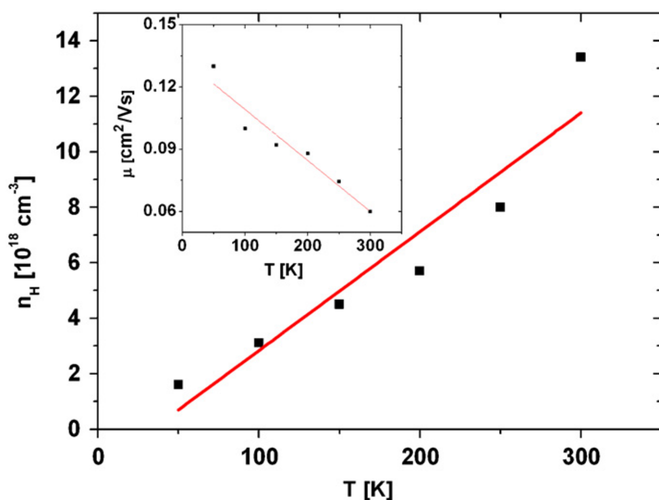

Fig. 5. The temperature dependence of Hall carrier concentration, n_H, and Hall mobility, μ_H, of GaN ceramic. The lines are guide for the eye.

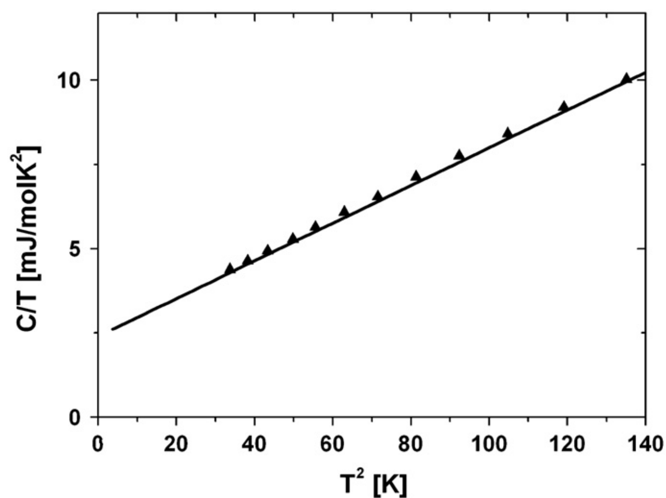

Fig. 6. Dependence of C/T vs. T^2 of GaN nanocrystalline ceramic measured at low temperatures.

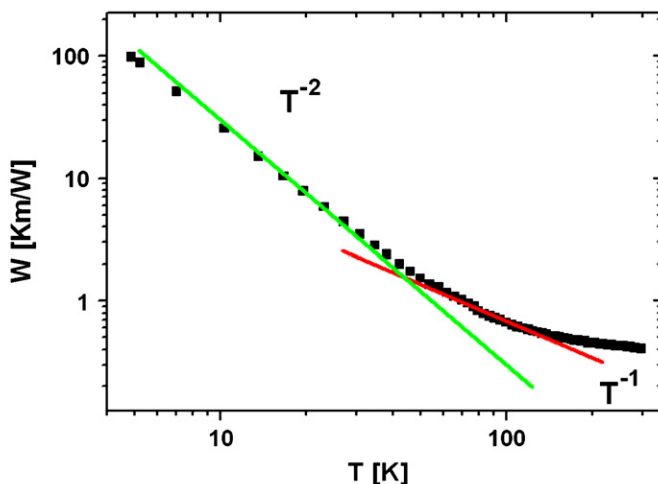

Fig. 7. The temperature dependence of thermal resistivity of GaN nanocrystalline ceramic.

The overall specific heat in low temperature range may be described by

$$C = C_e + C_l = \gamma T + A T^3, \quad (4)$$

which yields for our sample

$$C[\text{mJ/mol K}] = 2.4T + 58 \times 10^{-3} T^3. \quad (5)$$

From the data the Debye temperature has been determined to be 406 K.

3.6. Thermal resistivity

The temperature dependence of thermal resistivity of GaN ceramics is presented in Fig. 7. The thermal resistivity is a sum of different contributions $W_{tot} = \Sigma_i W_i$, arising from electron (W_e), phonon (W_{ph}) and bipolaron (W_{bip}) scattering.

All quantities in phonon contribution to heat transport are temperature dependent. At low temperatures $T \ll \Theta$, where Θ is Debye temperature, the phonons are scattered mainly at the boundaries of grains and $W_{ph} \sim T^{-3}$. At high temperatures ($T > \Theta$) the phonon–phonon scattering is dominant and thermal resistivity

satisfy $W_{ph}\sim T^{-1}$ (Leibfried–Schlömann). At intermediate temperatures i.e. $T>T_{max}$ (where T_{max} is temperature of maximal heat conductivity), Umklapp processes of phonon–phonon scattering prevail, which results in dependence $W_{ph}\sim \exp(-\Theta/3T)$.

The fitting of the sum with different contributions mentioned above indicated that dominance of two terms: one associated with the isolated dislocations and second originated in long range strains.

The discrepancy from the T^{-3} dependence for lowest temperatures ($T\ll\Theta$) results from scattering of phonons on grain boundaries and reflections with grain surfaces.

A plateau emerging at high temperatures may be ascribed to the amorphous part of sample which originates from high pressure and temperature sintering of ceramic. Theoretical considerations indicate that this plateau should occur at 10 K, however usually it is very weak and occurs at higher temperatures.

4. Conclusions

The electronic transport properties, heat capacity and thermal resistivity of GaN nanocrystalline ceramic prepared by hot pressing method at 4 GPa and relatively low temperature 450 °C have been investigated. Following the XRD measurements of GaN nanocrystalline powder and the respective ceramic it was concluded that it is composed from a small fraction of nanocrystals (13%) and amorphous part. The amorphous character of GaN ceramic was confirmed by very low thermal conductivity. It was found that the temperature dependence of resistivity clearly shows semiconducting behavior whereas other electronic properties, such as high charge carrier concentration and heat capacity place the GaN ceramics in group of semimetallic-like materials. The measured magnitude of resistivity was quite large because of extremely low electronic mobility which originates probably from high concentration of scattering centers. The weak electron–phonon interaction is pronounced by proportionality of Seebeck coefficient to temperature, which points out the diffusion mechanism as major contribution to Seebeck effect and negligible phonon-drag influence. The measured parameters of GaN ceramic make it attractive for application in opto-electronics.

In summary the GaN nanocrystalline ceramic was characterized by electronic transport properties (resistivity, thermopower and Hall effect) quite different in comparison to GaN crystalline forms (bulk crystals and films). The nature of electronic processes occurring in GaN ceramic is complex and associated with both semiconducting and semimetallic origins. One can conclude that amorphous phase of ceramic influences significantly the transport properties of GaN ceramic, especially by introducing additional energy levels in the band gap. Understanding the mechanisms responsible for high carrier concentration at simultaneous low electronic mobility in GaN ceramic needs further investigations in function of sintering parameters.

Acknowledgments

The ceramics were sintered at the Institute of High Pressure Physics of Polish Academy of Sciences in Warsaw due to courtesy of Prof. W. Lojowski.

References

[1] D. Hreniak, W. Strek, J. Amami, Y. Guyot, G. Boulon, C. Goutaudier, R. Pazik, J. Alloys Compd. 380 (2004) 348.
[2] Z. Zhao, V. Buscaglia, M. Viviani, M.T. Buscaglia, L. Mitoseriu, A. Testino, M. Nygren, M. Johnsson, P. Nanni, Phys. Rev. B 70 (2004) 024107.
[3] D. Hreniak, W. Strek, J. Alloys Compd. 341 (2002) 183.
[4] A. Krell, J. Klimke, T. Hutzler, J. Eur. Ceram. Soc. 29 (2009) 275.
[5] T. Omata, Y. Goto, S. Otsuka-Yao-Matsuo, Sci. Tech. Adv. Mater. 8 (2007) 524.
[6] I. Kosacki, C.M. Rouleau, P.F. Becher, J. Bentley, D.H. Lowndes, Solid State Ionics 176 (2005) 1319.
[7] K. Ando, Appl. Phys. Lett. 82 (2003) 100.
[8] T. Someya, R. Werner, A. Forchel, M. Catalano, R. Cingolani, Y. Arakawa, Science 285 (1999) 1905.
[9] J.C. Johnson, H.-J. Choi, K.P. Knutsen, R.D. Schaller, P. Yang, R.J. Saykally, Nat. Mater. 1 (2002) 106.
[10] A. Ponce, D.P. Bour, Nature 386 (1997) 351.
[11] A.J. Steckl, J.M. Zavada, Mater. Res. Soc. Bull. 24 (1999) 33.
[12] J. Simon, V. Protasenko, C. Lian, H. Xing, D. Jena, Science 327 (2010) 60.
[13] M. Nyk, W. Strek, J.M. Jablonski, L. Kepinski, R. Kudrawiec, J. Misiewicz, Mater. Sci. Semicond. Process 8 (2005) 511.
[14] M. Nyk, R. Kudrawiec, W. Strek, J. Misiewicz, Opt. Mater. 28 (2006) 767.
[15] R. Kudrawiec, M. Nyk, M. Syperek, A. Podhorodecki, J. Misiewicz, S. Strek, Appl. Phys. Lett. 88 (2006) 181916.
[16] W. Liu, A.A. Balandin, J. Appl. Phys. 97 (2005) 123705.
[17] Y.P. Xu, W.Y. Wang, D.F. Zhang, X.L. Chen, J. Mater. Sci. 36 (2001) 4401.
[18] F. Iskandar, T. Ogi, K Okuyama, Mater. Lett. 60 (2006) 73.
[19] L. Grocholl, J. Wang, E.G. Gillan, Chem. Mater. 13 (2001) 4290.
[20] C. Madhu, A. Sundaresan, C.N.R. Rao, Phys. Rev. B 77 (2008) 201306 R.
[21] T. Nishimura, M. Mitomo, H. Hirotsuru, M. Kawahara, J. Mater. Sci. Lett. 14 (1995) 1046.
[22] J. Li, Y. Ye, J. Am. Ceram. Soc. 89 (2006) 139.
[23] X.Y. Deng, X.H. Wang, Z.L. Gui, L.T. Li, I.W. Chen, J. Electroceram. 21 (2008) 238.
[24] R Fedyk, D Hreniak, W Łojkowski, W Strek, H Matysiak, E Grzanka, S Gierlotka, P. Mazur, Opt. Mater. 29 (2007) 252.
[25] A.J. Zaleski, M. Nyk, W. Strek, Appl. Phys. Lett. 90 (2007) 042511.
[26] P. Larson, S. Satpathy, Phys. Rev. B 76 (2007) 245205.
[27] C. Sulkowski, T. Klimczuk, R.J. Cava, K. Rogacki, Phys. Rev. B 76 (2007) 060501 R.
[28] R.B. Roberts, Philos. Mag. 36 (1977) 91.
[29] M. Ilegems, R. Dingle, J. Appl. Phys. 44 (1973) 4234.
[30] N.W. Ashcroft, N.D. Mermin, in: Solid State Physics, Harcourt, Orlando, 1976.
[31] S. Sergeenkov, F.M. Araujo-Moreira, J. Appl. Phys. 100 (2006) 096101.
[32] D.C. Look, J.R. Sizelove, S. Keller, Y.F. Wu, U.K. Mishra, S.P. DenBaars, Solid State Commun. 102 (1997) 297.